Updated Comparisons between Ground Radar and Satellite Precipitation Radar at Melbourne, Florida

Derek Podowitz
Georgia Institute of Technology
Department of Earth and Atmospheric Science
Atlanta, Georgia
Code 613.1

Mentor: Robert Meneghini
NASA Goddard Space Flight Center
Greenbelt, Maryland

Abstract: The objective of this paper is to update a study done by Liao and Meneghini. The study consists of a comparison between ground-based radar and satellite precipitation radar, the Weather Surveillance Radar-1988 Doppler (WSR-88D) and the Tropical Rainfall Measuring Mission (TRMM) precipitation radar (PR), respectively. The original study was done for a period from January 1998 to February 2007 and the updated period includes an additional 2 years and 8 months of data from January 1998 through October 2009. The update assesses how well the TRMM PR version 6 algorithms are working when compared to the WSR-88D. The focus of this study is to assess the bias between the reflectivities, correlation coefficients, and other statistical variables for PR and the ground validation (GV) for convective, stratiform, and all precipitation types. These precipitation types are compared with each other. Attenuation is important to take into account when comparing ground-based radar and satellite space-borne radar and needs to be corrected for a better comparison. It was shown that there was no significant difference in the statistics with the update. Once the version 7 algorithms are ready, this update will be ready to be compared for a more thorough study.

1. Introduction

The precipitation radar (PR) on the Tropical Rainfall Measuring Mission (TRMM) is the first active microwave instrument which measures three-dimensional structures that are primarily over the tropics and subtropics (Liao and Meneghini, 2009). The PR operates at a frequency of 13.8 GHz and is subject to attenuation from various forms of precipitation. Attenuation, in the case of the TRMM PR, increases as the signal penetrates deeper into the precipitation. This implies that as the height from the surface decreases, the difference between the attenuation-corrected and uncorrected radar reflectivities will increase. The ground validation (GV) for the TRMM PR is the Weather Surveillance Radar-1988 Doppler (WSR-88D) at Melbourne, FL which has an approximate frequency of 3 GHz. This location was selected because it is a well calibrated site with a large number of rain gauges in the vicinity from which the precipitation measurements can be validated. The purpose of this project was to update the data set for this study and to see how much of an effect this addition had on the statistics of the study. The original study contained 210 overpasses from January 1998 to February 2007. This update, from January 1998 to October 2009, nearly doubles the number of overpasses to 403. The data being assessed has already been corrected for attenuation.

The ground-based radar and satellite radar measure reflectivities on different coordinate which are represented in figure 1. When making this conversion, the curvature of the earth needs to be taken into account. For validating satellite data with ground-based data, both data sets need to be placed

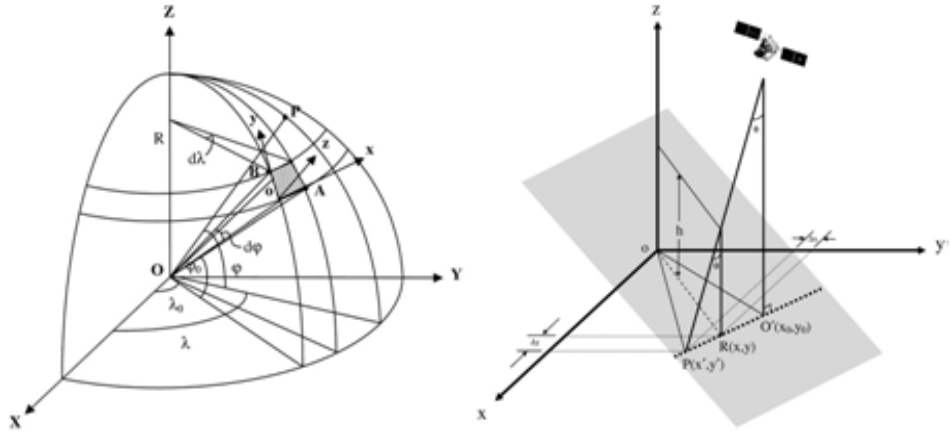

Figure 1 (a) represents a polar coordinate system for the earth's surface. (b) represents the satellite swatch path made the satellite.

on the same coordinate system and grid space. Figure 1a shows a polar coordinate system with respect to earth's shape and curvature. The satellite coordinate system and swath path, shown in figure 1b, are converted to the Cartesian coordinate system so that its points will be co-located on the same grid space as the ground radar. The common grid size which was used was $4 \times 4 \times 1.5$ km^3. The algorithms from the original study adjust for this difference. For a more thorough discussion on this conversion see the Liao-Meneghini 2009.

The following is the layout of this paper. The second section explains the data and methods used in the study. In the third section, the results from this updated study will be discussed. The final section provides a summary and offers insights into the use of the update for version 7 algorithms.

2. Data and Methods

In this study, the original data from January 1998 to February 2007 was rerun from January 1998 to December 2006 with a new criterion for indicating a corresponding overpass, which contains precipitation, to the radar site. This criterion defines when the TRMM satellite is within range of the Melbourne radar site. The fixed criterion is where the center of the sub-satellite ground track at nadir is within 175 kilometers of the center of the WSR-88D radar at the Melbourne site. A pixel will be displayed on the visuals of the radar or overpass if the percentage of precipitation in the ground radar is greater than 4%. A pixel in these visualizations represents one volume of space on the $4 \times 4 \times 1.5$ km^3 grid space, as mentioned previously. The criteria for corresponding overpasses are placed in algorithms to filter appropriate overpasses. Occasionally, some overpasses were overlooked and had to be added manually. Once all of the one-to-one ratios of the satellite PR overpass and ground-radar were accounted for, the corresponding files were used as inputs into Interactive Data Language (IDL) programs which output visualizations of the precipitation with respect to the WSR-88D radar and TRMM PR. With this new criterion, the number of corresponding overpasses increased from 210 overpasses to 299 overpasses. These 299 overpasses are a subset of the 403 overpasses and will be compared in the results.

The algorithms in this study extract the reflectivities and rain rate measured by the PR and the ground radar validation (GV). The reflectivities are measured at 1.5 km increments in the vertical plane beginning at 1.5 km and ending at 7.5 km. Tables 1 and 2 contain statistics for the mean reflectivities, the standard deviations, and the correlation between the PR and GV as well as the bias between them at different precipitation cases (convective, statiform, and total). Table 3 and 4 displays the rain-rate comparison between the PR and the GV.

3. Results

It was found that there was no significant difference between the statistics of the 1998-2006 sub-set and the updated data set. As can be seen from the visualizations in figure 2, TRMM PR does a relatively good job of detecting precipitation within its range. There are two notable differences between the WSR-88D and TRMM PR. First, the TRMM PR does not detect light precipitation in the lower atmosphere which is indicated by the blue areas in the WSR-88D visualizations. The other difference that can be seen in the maps is that the WSR-88D tends to show greater contrasts in the precipitation reflectivities of storms. By comparing these visualizations, one can see that TRMM PR has a tendency to overestimate the amount of precipitation. This is shown in the statistics seen in Tables 1 and 2. In both data sets the TRMM PR has a positive bias for all heights except for at 6 km. Why there is a negative bias at this height is unclear; however, it is known that there is a melting layer in the atmosphere at approximately 4-5 km from the surface. This is known to have an effect on

Table 3 displays the rain-rate comparison be

Figure 2 These four panels represent the output visualizations from IDL programs, quickView_2a25Overpass.pro and quickView_2a55ForTrmmOverpass.pro. The top precipitation readings are from the TRMM PR and the bottom reading are of the WSR-88D readings with an overlay of the TRMM overpass in gray. These figures are set to the same scale, where blue is at a 10 dBZ minimum and red is a 50 dBZ maximum

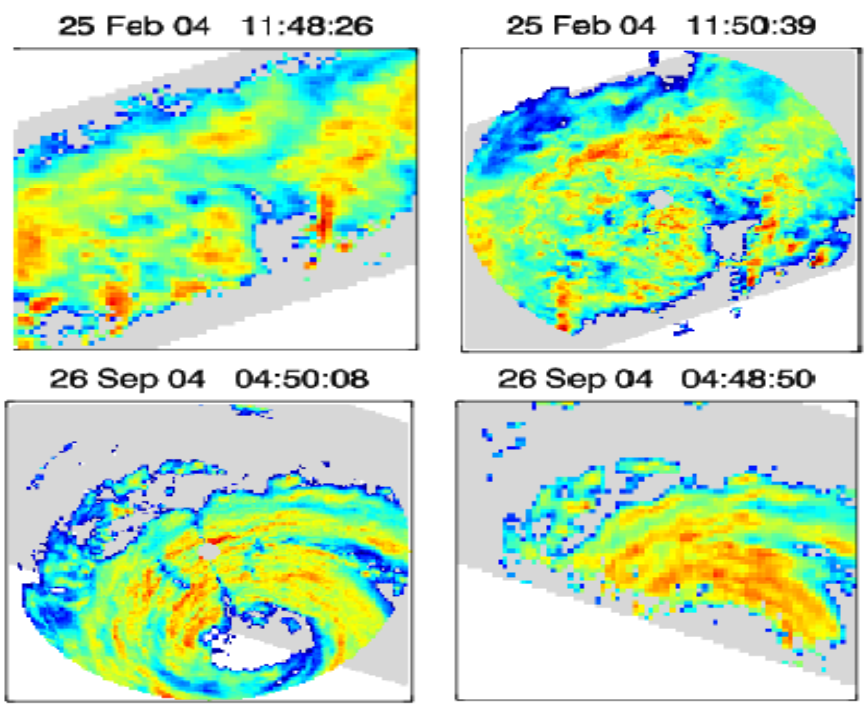

Table 1 The following statistics are for the rerun data from January 1998 to December 2006 for each 1.5 km height increment.

1998-2006 Convective Precipitation						
Height (km)	Mean PR reflectivity (Zpr)	σ (pr)	Mean GV reflectivity (Zgv)	σ (gv)	correlation coefficient (ρ)	bias (Zpr-Zgv)
1.5	33.76	6.99	33.69	7.94	0.783	0.07
3	33.79	7.22	33.48	7.94	0.818	0.31
4.5	30.92	7.25	30.75	7.64	0.830	0.17
6	26.71	6.1	26.98	6.71	0.809	-0.27
7.5	24.53	5.14	24.48	5.83	0.815	0.05
1998-2006 Stratiform Precipitation						
Height (km)	Mean PR reflectivity (Zpr)	σ (pr)	Mean ground radar (Zgv)	σ (gv)	correlation coefficient (ρ)	bias (Zpr-Zgv)
1.5	27.83	5.10	26.97	5.14	0.817	0.86
3	27.99	5.31	27.49	5.37	0.837	0.5
4.5	26.55	4.89	26.23	5.01	0.794	0.32
6	22.38	2.66	23.41	3.61	0.572	-1.03
7.5	21.43	1.99	21.15	2.48	0.603	0.28
1998-2006 Total Precipation						
Height (km)	Mean PR reflectivity (Zpr)	σ (pr)	Mean ground radar (Zgv)	σ (gv)	correlation coefficient (ρ)	bias (Zpr-Zgv)
1.5	29.59	6.37	29.00	6.86	0.836	0.59
3	29.57	6.48	29.15	6.76	0.854	0.42
4.5	27.79	6.02	27.52	6.24	0.831	0.27
6	24	4.80	24.74	5.32	0.773	-0.74
7.5	22.91	4.17	22.74	4.74	0.813	0.17

reflectivity measurements. For a 6 km height, a possible explanation for this negative bias is the non-Raleigh scattering at this height. This will be looked at in the future.

The above tables represent the statistics for the 1998 to 2006 subset. These values were calculated at each height increment in order to assess the validity of the Satellite Precipitation Radar compared to the ground radar. The Z_{pr} is the reflectivity of the TRMM PR which has been corrected for attenuation. The Z_{gv} is the reflectivity of the ground validation or WSR-88D ground radar. The Z-values in the table are the mean reflectivities over the 8 year period for the overpasses and ground radar. The σ_{pr} and σ_{gv} are the standard deviations of the mean values of the data. The correlation coefficient is the how well the PR and GV reflectivities match up with each other. The bias is the difference is the mean-values of the satellite precipitation radar and the ground validation radar.

The set of graphs in figure 3 are for the 1998 to 2006 subset at a height of 1.5 kilometers. The three graphs at the top are scatter-plots which display the correlation coefficient of the pixels with respect to the red line which represents the one-to-one ratio of the WSR-88D reflectivities to the TRMM PR reflectivities. The PR- and WSR-values are the average reflectivities in decibels of Z (dBZ) for the satellite precipitation radar and ground radar, respectively. The data points on the scatter-plot represent the pixels on the radar where precipitation was identified. The three bottom graphs are histograms which display the Probability Density Functions (PDFs) for the reflectivities of the precipitation radar which have been corrected for attenuation (represented by the black line), the measured reflectivi-

ties from the precipitation radar (represented by the black dotted line), and the reflectivities from the ground validation (represented by the blue dashed line).

In the previous study, the measured reflectivity (Z_m) from the TRMM PR was compared with the reflectivities of the corrected reflectivity (Z_{pr}) and ground radar reflectivity (Z_{gv}) (Liao and Meneghini, 2009). The histograms shown in Figures 3 through 6 show the probability density functions (PDFs) of the Z_m, Z_{pr}, and Z_{gv}. The PDFs for the corrected reflectivities are generally closer to the PDFs for the ground radar reflectivity than the PDFs for the measured reflectivities are to ground radar reflectivities. However, as the height increases from 1.5 km to 7.5 km, attenuation has less of an effect and the PDFs align more closely with each other.

Table 2 shows the same statistics as Table 1, but for the fully updated dataset from 1998 to 2009. Looking at the correlation coefficients and biases, it can be noted that there is a slight difference between corresponding statistics between the rerun 2006 dataset and the 2009 dataset. The correlation coefficients are within 5% (0.05) of each other which means that there is not a significant difference between the two datasets. The bias in this study is the difference between the mean reflectivities of the PR and the mean reflectivities of the GV (Z_{pr} - Z_{gv}). The biases for the two datasets for all the height increments seem are within 1 dBZ of each other which means that reflectivities of the ground radar and the space-borne radar correspond well.

Figure 3 The scatter-plots contain a comparison between the reflectivities of the ground and satellite precipitation radar for a height of 1.5 km for 299 overpasses in the 1998-2006 dataset. The red-line represents the one-to-one ratio of these reflectivities. Displayed on the scatter-plots are the correlation coefficient, the mean reflectivities of the satellite (PR) and ground radar (WSR), and the number of data points that correspond to the precipitation type. The histograms show the PDFs at this height.

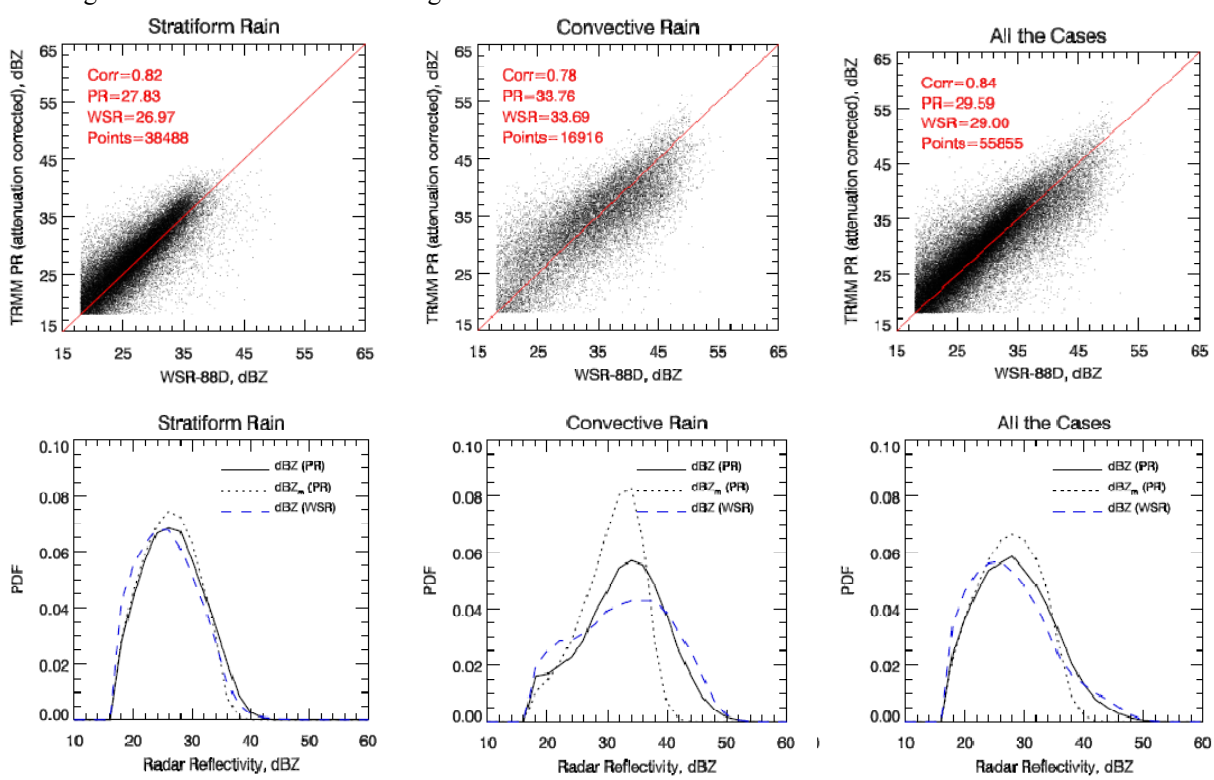

Table 2 This set of statistics are for the fully updated dataset from January 1998 to October 2009. The statistics are separated into stratiform, convective, and total precipitation types. The statistics were calculated at each 1.5 km increment from a height of 1.5 km to 7.5 km.

1998-2009 Convective Precipitation						
Height (km)	Mean PR reflectivity (Zpr)	σ (pr)	Mean GV reflectivity (Zgv)	σ (gv)	correlation coefficient (ρ)	bias (Zpr-Zgv)
1.5	33.87	6.88	33.72	7.99	0.767	0.15
3	33.78	7.15	33.46	7.98	0.807	0.32
4.5	30.98	7.19	30.79	7.68	0.819	0.19
6	26.68	6.12	26.97	6.76	0.803	-0.29
7.5	24.56	5.19	24.58	5.87	0.812	-0.02
1998-2009 Stratiform Precipitation						
Height (km)	Mean PR reflectivity (Zpr)	σ (pr)	Mean GV reflectivity (Zgv)	σ (gv)	correlation coefficient (ρ)	bias (Zpr-Zgv)
1.5	27.82	5.07	26.88	5.18	0.801	0.94
3	27.96	5.25	27.42	5.34	0.822	0.54
4.5	26.57	4.89	26.33	5.02	0.783	0.24
6	22.43	2.7	23.47	3.6	0.564	-1.04
7.5	21.4	1.98	21.17	2.45	0.584	0.23
1998-2009 Total Precipation						
Height (km)	Mean PR reflectivity (Zpr)	σ (pr)	Mean GV reflectivity (Zgv)	σ (gv)	correlation coefficient (ρ)	bias (Zpr-Zgv)
1.5	29.69	6.38	29.03	6.97	0.824	0.66
3	29.6	6.45	29.15	6.8	0.843	0.45
4.5	27.86	6.03	27.65	6.28	0.821	0.21
6	24.06	4.83	24.8	5.35	0.768	-0.74
7.5	22.93	4.22	22.82	4.79	0.811	0.11

a. Height comparisons

Figures 5 and 6 show how the statistics for the 1998-2009 dataset change from 1.5 km to the 3.0 km and 7.5 km heights.

These figures are being shown to give the reader an understanding of the statistics from tables 1 and 2. Although only examples from the 2009 dataset are shown in this paper, the same assessment was done for the 2006 dataset, as well.

The 3.0 height statistics contain more data points than the statistics at 1.5 km. Even so, the scatter-plots at both heights are similar to each other for all three precipitation types.

At a height of 7.5 km, the number of data points decrease and the correlation between the ground radar and satellite precipitation begin to decrease greatly for the stratiform precipitation to 0.58. The correlation coefficients for the convective and total type precipitation remain relatively the same throughout all the heights as seen in the data tables.

Figure 4 Shows the same statistical graphs as in figure 3 for a height of 1.5 km and the 403 overpasses from the 1998-2009 dataset.

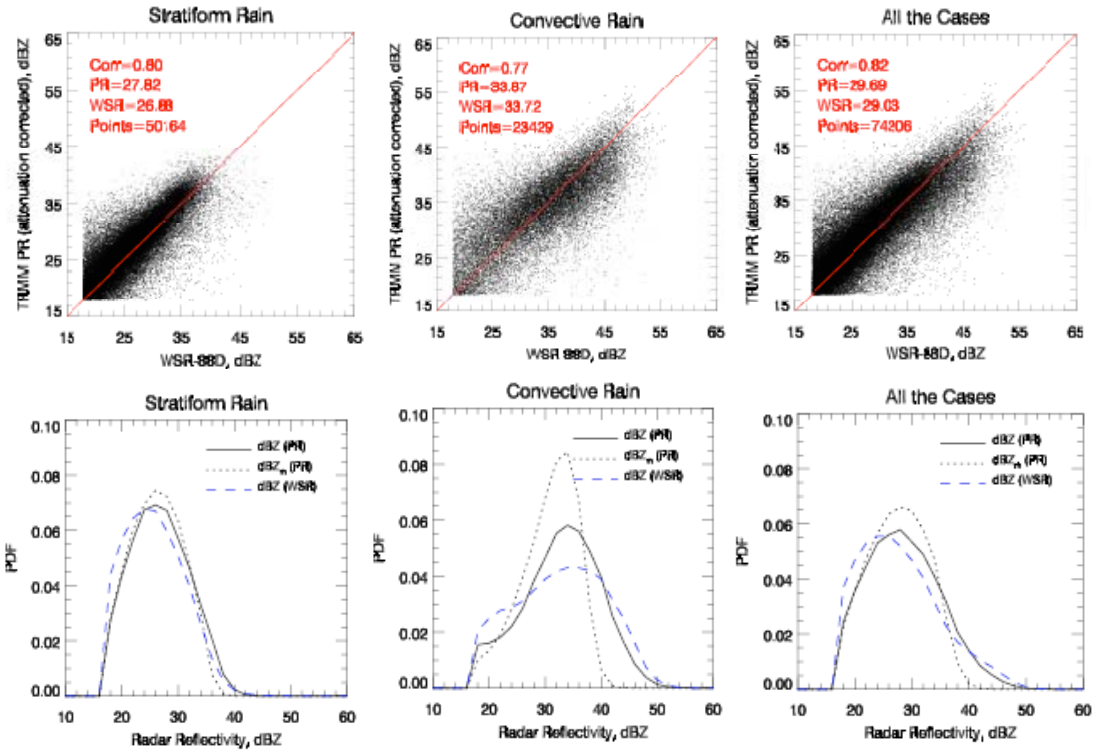

Figure 5 Shows the same statistical graphs and 2009 dataset as in figure 4 for a height of 3.0 km.

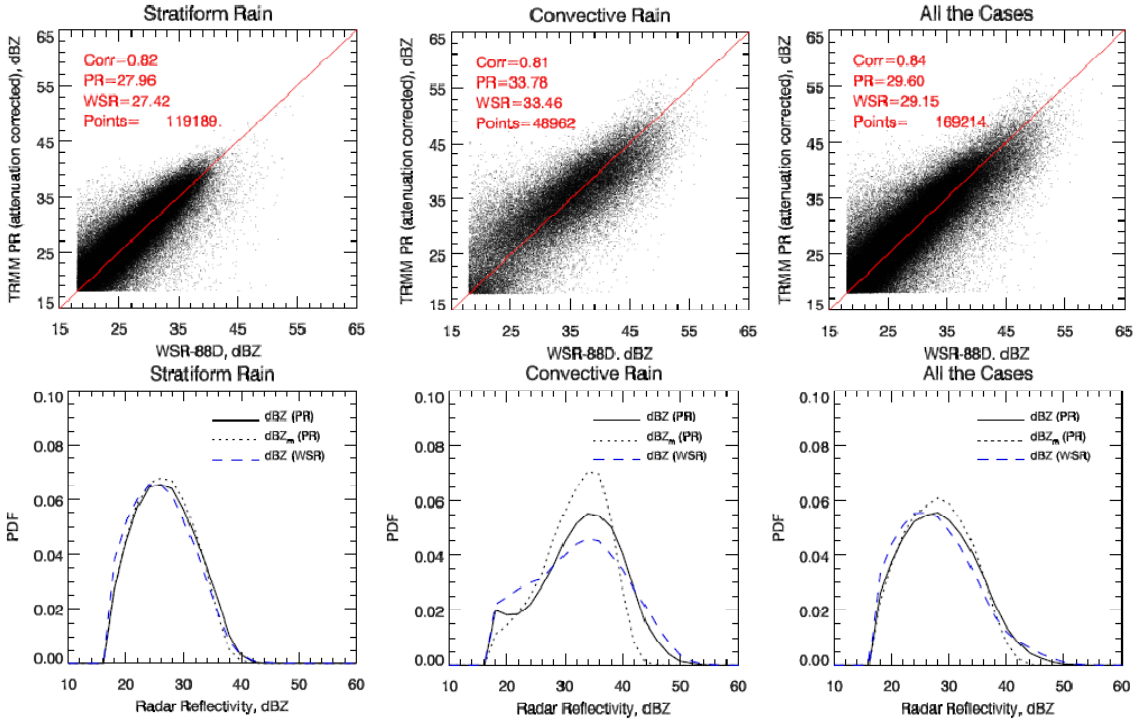

Figure 6 Shows the same statistical graphs and 2009 dataset as in figures 4 and 5for a height of 7.5 km.

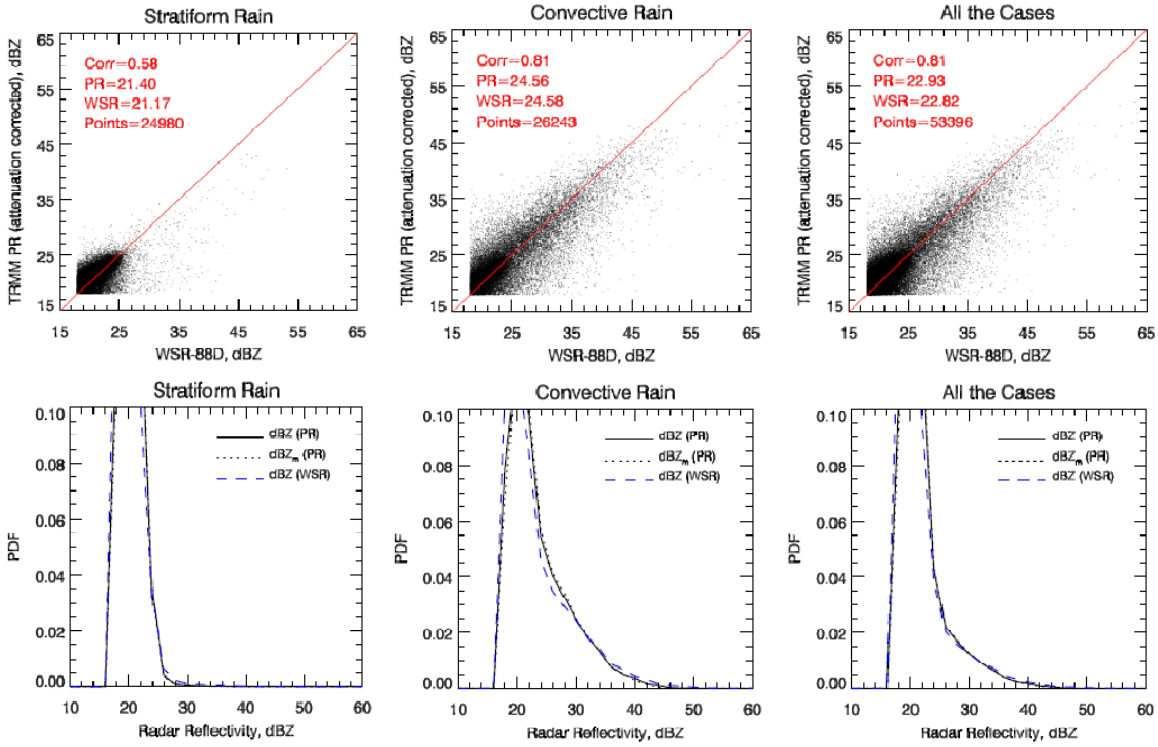

b. Rain rate comparisons

The algorithms used in this study take the reflectivities measured by the TRMM PR and WSR-88D and convert them to rain rates expressed in mm/hr. The data for the rain rates are taken for lower height levels near the surface.

The mean rain rates ($\bar{R}$) in tables 3 and 4 were calculated using the following equation:

$\bar{R} = \frac{1}{n}\sum_{i=1}^{n} R_i$, where n is the number of data points and R_i is the rain rate at a specified data point. The correlation coefficients for the rain rates are lower than those of the reflectivities.

The mean rain rates in figures 7 and 8 are measured in decibels of R (dBR); therefore, the equation used for this calculation is different (dBR = $10 \cdot \log_{10} R$). This was done because it scales down the R-values, so they are easier to interpret in a graphical format. The equation for these rain rates is as follows, $\overline{dBR} = \sum_{i=1}^{n} dBR_i$, where the same notations are used as in the previous equation.

In the scatter-plots for both datasets it can be seen that the rain rates for the stratiform and total precipitation types

Table 3 This table displays the rain rates from the 1998-2006 dataset whose statistics are separated into convective, statiform, and total precipitation types.

1998-2006 Rain Rate						
Case	Mean PR Rain Rate (Rpr)	σ (pr)	Mean GV Rain Rate (Rgv)	σ (gv)	correlation coefficient (ρ)	bias (Rpr-Rgv)
Convective	12.39	9.36	15.03	16.23	0.711	-2.64
Stratiform	4.24	4.68	3.9	3.95	0.682	0.34
Total	6.73	7.5	7.32	10.87	0.647	-0.59

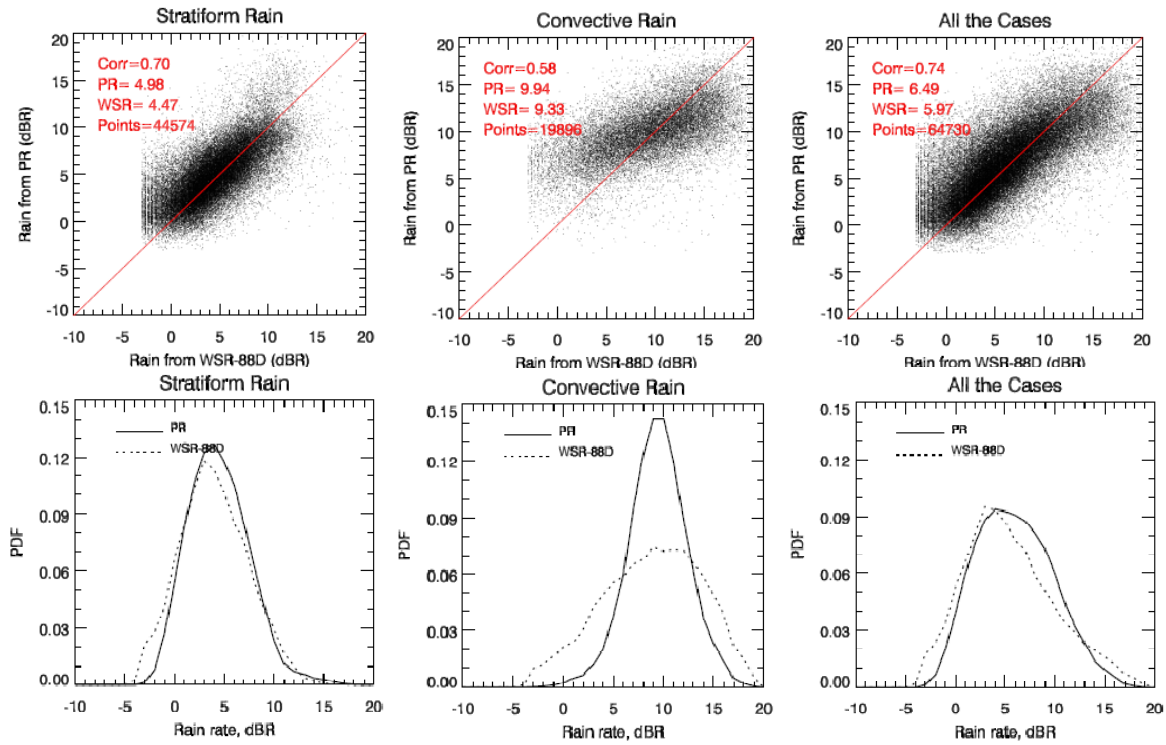

Figure 7 The scatter-plots contain a comparison between the rain rates of the ground and satellite precipitation radar in dBR for 299 overpasses in the 1998-2006 dataset. In this case, the red-line represents the one-to-one ratio of the rain rates for the PR and GV. Displayed on the scatter-plots are the correlation coefficient, the mean dBRs of the satellite (PR) and ground radar (WSR), and the number of data points that correspond to the precipitation type. The histograms show the PDFs for this dataset.

correspond well to each other. The PR and GV rain rates for the convective precipitation type, on the other hand, do not correlate as well. This is validated in the statistics shown in tables 3 and 4 as well as in the histograms from figures 7 and 8. In the convective type histograms, where the solid black line represents the PDF for the TRMM PR rain rates and the dotted black line represents the PDF for the WSR-88D rain rates, show a clear discrepancy. The biases for the convective precipitation in the 1998-2006 dataset (-2.64) and the 1998-2009 dataset (-3.01) are greater than 1 dBR and therefore, there is a significant difference in the statistics which will need to be corrected for in the future.

The next set of graphs in figure 9 show the area-averaged rain rate for the 1998-2006 dataset (figure 9a) and for the 1998-2009 dataset (figure 9b). Each data point represents the area-averaged rain rate for an overpass, so figure 9a contains 299 data points and figure 9b contains 403 data points. These graphs also show the correlation between the area-average rain

Table 4 This table displays the rain rates from the 1998-2009 dataset whose statistics are separated into convective, statiform, and total precipitation types.

1998-2009 Rain Rate						
Case	Mean PR Rain Rate (Rpr)	σ (pr)	Mean GV Rain Rate (Rgv)	σ (gv)	correlation coefficient (ρ)	bias (Rpr-Rgv)
Convective	12.06	8.93	15.07	16.3	0.691	-3.01
Stratiform	4.15	4.36	3.94	4.05	0.653	0.21
All	6.67	7.22	7.51	11.1	0.603	-0.84

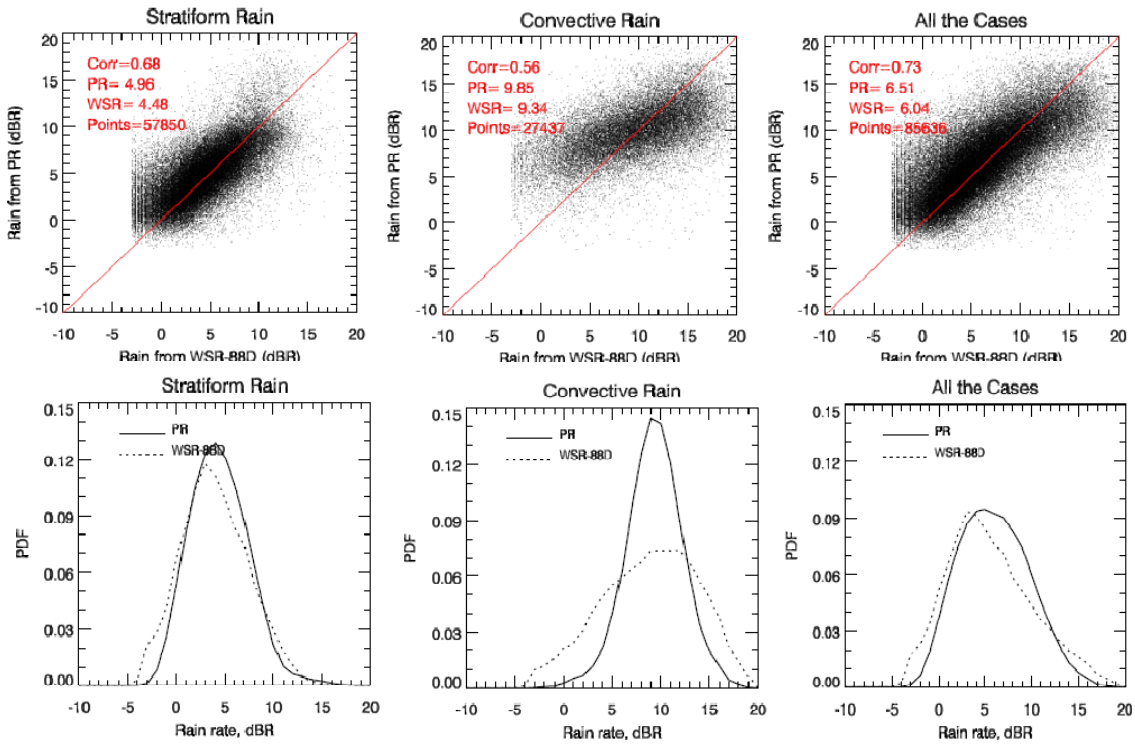

Figure 8 Shows the same statistical graphs as in figure 7 for the 403 overpasses from the 1998-2009 dataset.

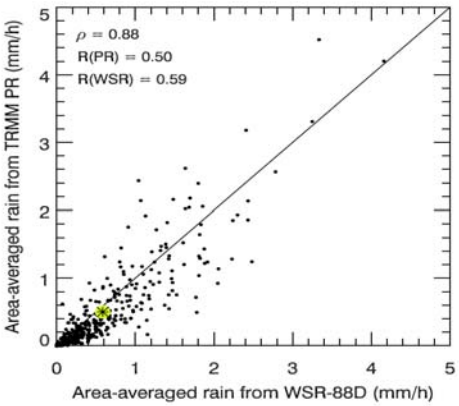

a.

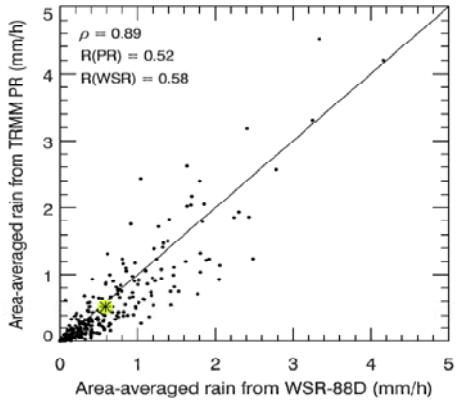

b.

Figure 9 on the left shows the area-average rain comparison where (a) is the area-averaged rain rate for the 1998-2006 dataset and (b) is the area-averaged rain rate for the 1998-2009 dataset. The data point marked by an asterisk highlighted in yellow is the overall average of all the overpasses for each dataset.

rates for the PR and the GV which seem to correlate well in both datasets. To understand how the area-averaged rain rate is computed, please refer to the Liao-Meneghini 2009 paper.

4. Conclusion

Upon final assessment of this study, it was found that, even with a substantial increase in the number of corresponding overpasses, there was no significant difference in the statistics for the rerun 1998 to 2006 dataset and the updated 1998 to 2009 dataset.

A supplementary study was done to compute the root mean square error for the ground radar which assess beam-filling

issues and any possible error that may occur with an increase in distance from the radar. It was hypothesized that the error would increase with distance; however, it was found that the error did not change significantly with distance.

For the rest of the study, further consideration needs to be taken for the discrepancies in the correlation between the PR and GV for stratiform type precipitation at higher heights. Another possible assessment to look into would be the negative bias shown in the 6.0 km height levels. Lastly, the correlation between the PR and GV rain rates for convective precipitation could be looked at more thoroughly, as well.

Overall, this update was an important step that needed be taken to validate the version 6 satellite algorithms, so that when version 7 comes out, the comparison can be done.

Acknowledgements I would like to thank my mentor Dr. Robert Meneghini for all his help and Summer Institute in Earth Science for providing me with this opportunity.

References: Liao, L., R. Meneghini, 2009: Validation of TRMM Precipitation Radar through Comparison of Its Multiyear Measurements with Ground-Based Radar. *J. Appl. Meteor.*, **44**, 804-817.

Glossary:
Nadir: The center point or zenith angle of a satellite's path.

Appendix:
List of programs and algorithms used for study:
quickView_2a25Overpass.pro
quickView_2a55ForTrmmOverpass.pro
comparison_PRv6_GV_dBZ_v2.pro
plot_scaPoint_landscape_v2.pro
plot_histogram_landscape_v2.pro
comparison_PRv6_GV_RAIN_v2.pro
plot_scaPoint_rain_landscape_v2.pro
plot_histogram_rain_landscape_v2.pro
comparison_2a25_2a53_PRv6_areaAvg_rain_v2.pro
plot_scaPoint_pr_gv_areaAvgRain.pro

Created programs and algorithms for study:
plot_total_dist_vs_rms.pro
plot_stratiform_dist_vs_rms.pro
plot_convective_dist_vs_rms.pro
compdata.f90